DOI: 10.1002/ejic.200900353

Syntheses, Structures and Magnetic Properties of Heterobridged Dinuclear and Cubane-Type Tetranuclear Complexes of Nickel(II) Derived from a Schiff Base Ligand

Susanta Hazra,[a] Rajesh Koner,[a] Pascale Lemoine,[b] E. Carolina Sañudo,*[c] and Sasankasekhar Mohanta*[a]

Keywords: Magnetic properties / Bridging ligands / Schiff bases / Cage compounds / Structure elucidation

Syntheses, structures and magnetic properties of a heterobridged μ-phenoxido-$\mu_{1,1}$-NCO dinickel(II) compound $[Ni^{II}_2(HL)_3(\mu\text{-}NCO)]\cdot 2H_2O$ (**1**) and a heterobridged bis(μ_3-phenoxido)bis(μ_3-alkoxido)tetranickel(II) system, $[Ni^{II}_4(L)_2(HL)_2(SeCN)_2(H_2O)_2]\cdot C_3H_7NO\cdot 4H_2O$ (**2**), containing a cubane-type $Ni^{II}_4O_4$ core, derived from the tetradentate Schiff base compartmental ligand *N*-(2-hydroxyethyl)-3-methoxysalicylaldimine (H_2L) were described. Compounds **1** and **2** crystallize in triclinic $P\bar{1}$ and monoclinic $P2_1/c$ systems, respectively. Compound **2**, in which the Ni_4O_4 cubane core is composed of two μ_3-phenoxido and two μ_3-alkoxido moieties, represents the sole example of this type. The variable-temperature (2–300 K) magnetic susceptibilities and magnetizations of these two compounds were measured. The interaction between the metal centres in dinuclear compound **1** is weak ferromagnetic, resulting in an $S_T = 2$ ground state at 2 K. The overall interaction observed in **2** is weak ferromagnetic, leading to an unusual $S_T = 3$ ground state.

Introduction

Studies of the magnetic properties of exchange-coupled compounds have attracted much attention to understand the intimate role of spin coupling and to develop molecule-based magnetic materials.[1–7] As most of the reported exchange-coupled compounds are antiferromagnetically coupled,[1] designed synthesis of systems exhibiting ferromagnetic interaction is an important task.

Heterobridged μ-hydroxido/alkoxido/phenoxido-μ-X (X = azide, thiocyanate, cyanate, pyrazolate, carboxylate, 7-azaindolate, etc.) compounds can be considered as a special class of exchange-coupled systems because of the involvement of two pathways to govern the overall nature and magnitude of superexchange interaction.[1a,6–8] Magnetic properties of heterobridged μ-hydroxido/alkoxido/phenoxido-μ-X dicopper(II) compounds have been extensively investigated and the mechanism of interaction has been understood by the concept of orbital complementarity and coutercomplementarity.[1a,6] In contrast, magnetic properties of μ-hydroxido/alkoxido/phenoxido-μ-X compounds of other 3d metal ions have not been explored much and therefore this area deserves more attention.[7,8]

As mentioned, one aim in molecular magnetism is to develop magnetic materials that obviously exhibit spontaneous magnetization at higher temperatures. Except for a few dinuclear 3d–4f compounds,[4a] spontaneous magnetization has been observed in assembled systems, polymeric or large spin clusters.[4,5] Therefore, designed synthesis and studies of magnetic properties of exchange-coupled clusters is an important aspect.

Tetranickel(II) complexes having a Ni_4O_4 cubane-like core have attracted much attention.[9–21] For compounds of this type, the diamagnetic singlet state ($S_T = 0$) and maximum spin containing nonate state ($S_T = 4$) are the frequently observed ground states. Recent observation of single molecular magnetic properties in some of the Ni_4O_4 cubane compounds[9c,9d] indicates that these types of systems should be explored more to develop magnetic materials.

The Schiff base ligand (H_2L; Scheme 1)[22] obtained upon condensation of 3-methoxysalicylaldehyde and ethanolamine is in principle a tetradentate ligand. However, the coordination ability of the ether oxygen atom to 3d metal ions is not high, and hence, in practice it will behave as a tridentate ligand. Therefore, we anticipated that the combined effect of H_2L and a pseudohalide may stabilize het-

[a] Department of Chemistry, University of Calcutta, 92 A. P. C. Road, Kolkata 700009, India
Fax: +91-33-23519755
E-mail: sm_cu_chem@yahoo.co.in
[b] Université Paris Descartes, Laboratoire de Cristallographie et RMN biologiques UMR 8015, Faculté de Pharmacie, 4 avenue de l'Observatoire, 75006 Paris, France
[c] Department de Química Inorgànica i Institut de Nanociència i Nanotecnologia, Universitat de Barcelona, Diagonal 647, 08028 Barcelona, Spain
E-mail: carolina.sanudo@qi.ub.es
Supporting information for this article is available on the WWW under http://dx.doi.org/10.1002/ejic.200900353.

erobridged μ-phenoxido-μ-pseudohalide dimetal systems. We also anticipated that if, in addition to the phenoxido moiety, the alcohol moiety could be deprotonated, a possibility to derive a high nuclearity cluster as a result of the simultaneous bridging of both the phenoxido and alkoxido groups might arise. In either of the heterobridged cases, μ-phenoxido-μ-pseudohalide or μ-phenoxido-μ-alkoxido, the derived systems may be ferromagnetically coupled if the bridge angles are close to the angle required for orthogonality. With these aims, the reactions between nickel(II) salt and H_2L in the presence of a base and cyanate or selenocyanate were carried out. Whereas a heterobridged μ-phenoxido-μ-pseudohalide dinickel(II) compound $[Ni^{II}_2(HL)_3(\mu_{1,1}\text{-NCO})]\cdot 2H_2O$ (**1**) was isolated, the product containing selenocyanate was a cubane-type heterobridged bis(μ_3-phenoxido)bis(μ_3-alkoxido) tetranuclear system $[Ni^{II}_4(L)_2(HL)_2(SeCN)_2(H_2O)_2]\cdot C_3H_7NO\cdot 4H_2O$ (**2**), in which two selenocyanate moieties behave as terminal ligands to two different metal ions. We report here the syntheses, structures and magnetic properties of these two compounds **1** and **2**.

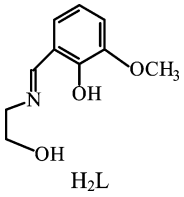

Scheme 1. Chemical structure of H_2L.

Results and Discussion

Syntheses and Characterization

The dinuclear nickel(II) complex $[Ni^{II}_2(HL)_3(\mu_{1,1}\text{-NCO})]\cdot 2H_2O$ (**1**) is readily obtained in high yield from the reaction of the H_2L ligand, nickel(II) perchlorate hexahydrate, triethylamine and NaOCN in a 3:2:6:2 ratio. Similarly, the reaction of H_2L, nickel(II) perchlorate hexahydrate, triethylamine and KSeCN in a 1:1:2:0.8 ratio produces tetranickel(II) compound **2** in high yield. In **1**, only the phenoxido groups of the three ligands are deprotonated. Among the four ligands in **2**, two are monodeprotonated, in which the phenoxido oxygen is deprotonated, and both the phenol and alcohol groups are deprotonated for the other two ligands.

The IR spectrum of the free H_2L ligand exhibits one strong absorption band at 1644 cm^{-1} due to a $\nu_{C=N}$ vibration.[22] In both complexes **1** and **2**, the vibration due to $\nu_{C=N}$ appears in a slightly lower region (1637 cm^{-1} for **1** and 1630 cm^{-1} for **2**). The presence of isocyanate in **1** and selenocyanate in **2** is evidenced by the appearance of a very strong signal at 2181 and 2112 cm^{-1}, respectively. The stretching mode for water for both complexes is observed as a broad band at 3396 and 3334 cm^{-1} for **1** and **2**, respectively.

Description of the Structure of Compound 1

The structure of $[Ni^{II}_2(HL)_3(\mu_{1,1}\text{-NCO})]\cdot 2H_2O$ (**1**; Figure 1) consists of two nickel(II) centres that are bridged by a phenoxido moiety and an end-on ($\mu_{1,1}$-N) isocyanate ion. Of the three phenolate oxygen atoms, O(2) is coordinated to Ni(1) and O(42) to Ni(2), whereas O(22) bridges the two metal centres. The two imino nitrogen atoms, N(8) and N(28), are coordinated to Ni(1), whereas only N(48) is coordinated to Ni(2). Again, of the three alcoholic oxygen atoms, O(10) is coordinated to Ni(1) and O(50) to Ni(2), whereas O(30) remains uncoordinated. Interestingly, the hexacoordination of the Ni(2) centre is achieved through the coordination of methoxy oxygen O(20). Thus, in **1** the three ligands are bonded differently to the two metal centres.

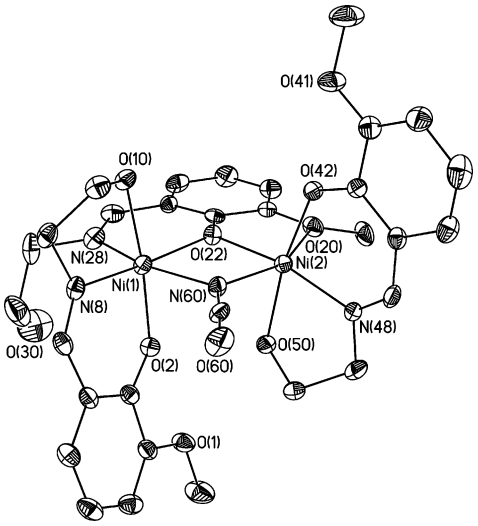

Figure 1. Crystal structure of $[Ni^{II}_2(HL)_3(\mu\text{-NCO})]\cdot 2H_2O$ (**1**). Hydrogen atoms and water molecules are omitted for clarity.

In the case of Ni(1), the best plane is provided by N(8) N(28)O(22)N(60), whereas in the case of Ni(2) the equatorial plane is defined by O(22)N(60)N(48)O(20). The average deviation of the constituent atoms from their least-squares planes in the two cases is 0.07 and 0.10 Å, whereas the Ni(1) and Ni(2) atoms are displaced from their respective basal planes by 0.08 and 0.15 Å. Clearly, the two metal centres lack ideal coordination geometry. For both metal centres, the axial positions are occupied by a phenolate oxygen atom [O(2) for Ni(1) and O(42) for Ni(2)] and an alcohol oxygen atom [O(10) for Ni(1) and O(50) for Ni(2)]. The bridge angles Ni(1)–O(22)–Ni(2) and Ni(1)–N(60)–Ni(2) involving the phenoxide and isocyanate are 106.5(2) and 94.1(2)°, respectively. The dihedral angle between these two bridges is 15.7°, whereas the separation between the metal centres is 3.182 Å.

A consideration of the bond lengths given in Table 1 reveals that while the phenoxido bridged Ni–O distances are almost identical [Ni(1)–O(22) 1.982(5) Å, Ni(2)–O(22)

1.990(5) Å], the two isocyanate-bridged Ni–N distances are unequal [Ni(1)–N(60) 2.236(6) Å, Ni(2)–N(60) 2.111(7) Å]. The two Ni–O(alcohol) distances are not much different [Ni(1)–O(10) 2.111(5) Å, Ni(2)–O(50) 2.149(5) Å], as are the two Ni–O(phenolate) distances [Ni(1)–O(2) 2.015(5) Å, Ni(2)–O(42) 1.977(5) Å]. Again, the two imine Ni–N distances are quite similar [Ni(1)–N(8) 1.995(6) Å, Ni(2)–N(48) 1.971(7) Å]. In contrast, the bond length involving imine nitrogen N(28) to Ni(1) [2.077(7) Å] is longer. The unusually coordinating methoxy oxygen O(20) is rather weakly bonded to Ni(2) [2.266(6) Å].

Table 1. Selected bond lengths [Å] and angles [°] for **1**.

Ni(1)–O(10)	2.111(5)	Ni(2)–O(50)	2.149(5)
Ni(1)–O(2)	2.015(5)	Ni(2)–O(42)	1.977(5)
Ni(1)–O(22)	1.982(5)	Ni(2)–O(22)	1.990(5)
Ni(1)–N(60)	2.236(6)	Ni(2)–N(60)	2.111(7)
Ni(1)–N(8)	1.995(6)	Ni(2)–N(48)	1.971(7)
Ni(1)–N(28)	2.077(7)	Ni(2)–O(20)	2.266(6)
O(2)–Ni(1)–O(10)	172.0(2)	O(42)–Ni(2)–O(50)	170.9(2)
N(8)–Ni(1)–O(22)	167.7(3)	O(22)–Ni(2)–N(48)	165.6(3)
N(28)–Ni(1)–N(60)	166.6(3)	O(20)–Ni(2)–N(60)	154.8(2)
O(2)–Ni(1)–O(22)	95.8(2)	O(42)–Ni(2)–O(22)	102.6(2)
O(2)–Ni(1)–N(8)	92.1(3)	O(42)–Ni(2)–N(48)	91.6(3)
O(2)–Ni(1)–N(60)	87.7(2)	O(42)–Ni(2)–N(60)	95.0(2)
O(2)–Ni(1)–N(28)	93.6(3)	O(42)–Ni(2)–O(20)	89.7(2)
O(10)–Ni(1)–O(22)	92.0(2)	O(50)–Ni(2)–O(22)	85.9(2)
O(10)–Ni(1)–N(8)	79.9(3)	O(50)–Ni(2)–N(48)	79.7(3)
O(10)–Ni(1)–N(60)	92.4(2)	O(50)–Ni(2)–N(60)	89.4(2)
O(10)–Ni(1)–N(28)	88.2(2)	O(50)–Ni(2)–O(20)	89.7(2)
N(60)–Ni(1)–N(8)	93.5(2)	N(60)–Ni(2)–O(22)	80.3(2)
N(60)–Ni(1)–O(22)	77.4(2)	N(60)–Ni(2)–N(48)	101.3(3)
N(28)–Ni(1)–N(8)	99.8(3)	O(20)–Ni(2)–O(22)	74.5(2)
N(28)–Ni(1)–O(22)	89.2(3)	O(20)–Ni(2)–N(48)	103.4(3)
Ni(1)–O(22)–Ni(2)	106.5(2)	Ni(1)–N(60)–Ni(2)	94.1(2)

Distortions of the two nickel centres from ideal octahedral geometry are reflected in their *trans* angles, which vary between 166.6(3) and 172.0(2)° for Ni(1) and between 154.8(2) and 170.9(2)° for Ni(2). Obviously, the geometry of Ni(2) deviates far from a regular octahedral environment. The ranges of the *cis* angles [77.4(2)–99.8(3)° for Ni(1) and 74.5(2)–103.4(3)° for Ni(2)] are also indicative of the greater distortion of the Ni(2) coordination environment.

There are a number of hydrogen-bonding interactions involving water molecules, phenoxido, methoxy, alcohol and isocyanate oxygen atoms and one C–H moiety. A 2D network resulting from all these hydrogen bridges is shown in Figure S1 (Supporting Information).

Description of the Structure of Compound 2

The crystal structure of $[Ni^{II}_4(L)_2(HL)_2(SeCN)_2(H_2O)_2]\cdot C_3H_7NO\cdot 4H_2O$ (**2**) is shown in Figure 2. As may be noted, this is a cubane-type structure consisting of four nickel(II) centres, two monodeprotonated ligands $[HL]^-$, in which the phenoxido moiety is deprotonated, two dideprotonated ligands $[L]^{2-}$, in which both the phenol and alcohol moieties are deprotonated, two monodentate selenocyanate units acting as terminal ligands and two coordinated water molecules. Compound **2** contains four solvated water molecules as well as an *N*,*N*′-dimethylformamide molecule. Of the four phenolate oxygen atoms, O(12) and O(22) behave as a μ_3-bridging centre, whereas O(2) and O(32) are coordinated terminally. Again, the alkoxido oxygen atoms O(10) and O(40) are μ_3-bridging, whereas the nondeprotonated alcohol oxygen atoms O(20) and O(30) remain uncoordinated. In Figure 3, a simplified representation of the coordination environments around the four metal centres is given.

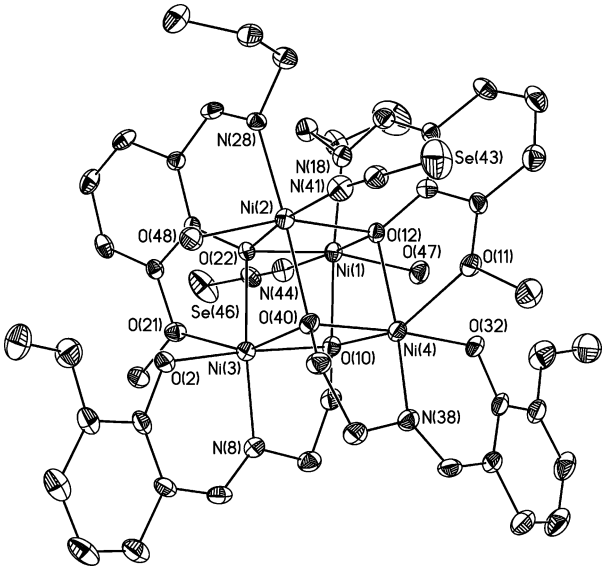

Figure 2. Crystal structure of $[Ni^{II}_4(L)_2(HL)_2(SeCN)_2(H_2O)_2]\cdot C_3H_7NO\cdot 4H_2O$ (**2**). Hydrogen atoms, water and dmf molecules are omitted for clarity.

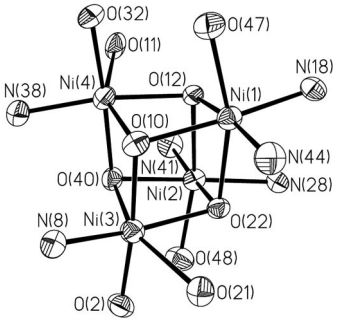

Figure 3. Simplified representation of the coordination environment of the four metal centres in $[Ni^{II}_4(L)_2(HL)_2(SeCN)_2(H_2O)_2]\cdot C_3H_7NO\cdot 4H_2O$ (**2**).

The coordination environments of Ni(1) and Ni(2) are similar. Ni(1) is coordinated with μ_3-phenoxido oxygen atoms O(12) and O(22), μ_3-alkoxido oxygen O(10), imine nitrogen N(18), selenocyanate nitrogen N(44) and water oxygen O(47). Similarly, Ni(2) is bonded to the μ_3-phenoxido oxygen atoms O(12) and O(22), μ_3-alkoxido oxygen O(40), imine nitrogen N(28), selenocyanate nitrogen N(41) and water oxygen O(48). For the six-coordinate metal centres, the basal planes for Ni(1) and Ni(2) are defined by N(18)N(44)O(10)O(12) and N(28)N(41)O(40)O(22), respectively. The average deviations of the constituent atoms from

the respective planes are 0.06 and 0.04 Å, whereas the metal ions are displaced by 0.08 and 0.09 Å from the least-squares planes. The bond lengths given in Table 2 indicate that for similar donor atoms the bond lengths for Ni(1) and Ni(2) are comparable. It may be noted that for both Ni(1) and Ni(2) the apical bond length involving a phenoxido oxygen [O(22) for Ni(1) and O(12) for Ni(2)] is significantly longer [2.265(4) Å for Ni(1) and 2.281(4) Å for Ni(2)] than the remaining other five bond lengths [2.007(6)–2.069(5) Å for Ni(1) and 2.023(6)–2.075(4) Å for Ni(2)]. For the Ni(1) and Ni(2) coordination environment the *trans* angles lie between 161.01(17) and 171.68(19)° and the *cis* angles range between 75.81(15) and 103.76(16)°. Taken together with their bond lengths, Ni(1) and Ni(2) represent a distorted octahedral geometry.

Table 2. Selected bond lengths [Å] and angles [°] for **2**.

Ni(1)–O(22)	2.265(4)	Ni(2)–O(12)	2.281(4)
Ni(1)–O(47)	2.069(5)	Ni(2)–O(48)	2.043(5)
Ni(1)–O(10)	2.063(4)	Ni(2)–O(40)	2.075(4)
Ni(1)–O(12)	2.046(4)	Ni(2)–O(22)	2.043(4)
Ni(1)–N(18)	2.069(5)	Ni(2)–N(28)	2.065(5)
Ni(1)–N(44)	2.007(6)	Ni(2)–N(41)	2.023(6)
Ni(3)–O(21)	2.279(4)	Ni(4)–O(11)	2.301(4)
Ni(3)–O(40)	2.090(4)	Ni(4)–O(10)	2.090(4)
Ni(3)–O(2)	1.959(4)	Ni(4)–O(32)	1.968(4)
Ni(3)–N(8)	1.971(5)	Ni(4)–N(38)	1.968(5)
Ni(3)–O(10)	2.042(4)	Ni(4)–O(40)	2.025(4)
Ni(3)–O(22)	2.038(4)	Ni(4)–O(12)	2.048(4)
O(22)–Ni(1)–O(47)	161.75(19)	O(12)–Ni(2)–O(48)	161.01(17)
O(10)–Ni(1)–N(18)	169.73(18)	O(40)–Ni(2)–N(28)	168.54(18)
O(12)–Ni(1)–N(44)	171.4(2)	O(22)–Ni(2)–N(41)	171.68(19)
O(22)–Ni(1)–O(10)	76.94(14)	O(12)–Ni(2)–O(40)	75.81(15)
O(22)–Ni(1)–O(12)	76.36(14)	O(12)–Ni(2)–O(22)	76.03(14)
O(22)–Ni(1)–N(18)	100.46(16)	O(12)–Ni(2)–N(28)	99.20(17)
O(22)–Ni(1)–N(44)	95.03(19)	O(12)–Ni(2)–N(41)	95.87(18)
O(47)–Ni(1)–O(10)	87.97(19)	O(48)–Ni(2)–O(40)	88.50(18)
O(47)–Ni(1)–O(12)	91.8(2)	O(48)–Ni(2)–O(22)	91.44(19)
O(47)–Ni(1)–N(18)	92.6(2)	O(48)–Ni(2)–N(28)	94.2(2)
O(47)–Ni(1)–N(44)	96.5(2)	O(48)–Ni(2)–N(41)	95.9(2)
O(10)–Ni(1)–O(12)	82.89(15)	O(22)–Ni(2)–O(40)	81.96(15)
O(10)–Ni(1)–N(44)	95.2(2)	O(40)–Ni(2)–N(41)	94.32(19)
O(12)–Ni(1)–N(18)	86.85(19)	O(22)–Ni(2)–N(28)	86.84(18)
N(18)–Ni(1)–N(44)	94.9(2)	N(28)–Ni(2)–N(41)	96.5(2)
O(21)–Ni(3)–O(40)	154.73(16)	O(10)–Ni(4)–O(11)	154.82(16)
O(22)–Ni(3)–N(8)	161.3(2)	O(12)–Ni(4)–N(38)	161.8(2)
O(2)–Ni(3)–O(10)	173.34(18)	O(32)–Ni(4)–O(40)	174.55(18)
O(21)–Ni(3)–O(2)	86.14(17)	O(11)–Ni(4)–O(32)	85.81(17)
O(21)–Ni(3)–N(8)	96.07(19)	O(11)–Ni(4)–N(38)	97.56(19)
O(21)–Ni(3)–O(10)	100.21(15)	O(11)–Ni(4)–O(40)	99.02(16)
O(21)–Ni(3)–O(22)	73.80(15)	O(11)–Ni(4)–O(12)	73.25(15)
O(40)–Ni(3)–O(2)	92.58(17)	O(10)–Ni(4)–O(32)	93.78(17)
O(40)–Ni(3)–N(8)	109.19(19)	O(10)–Ni(4)–N(38)	107.60(19)
O(40)–Ni(3)–O(10)	82.53(15)	O(10)–Ni(4)–O(40)	82.95(15)
O(40)–Ni(3)–O(22)	81.72(15)	O(10)–Ni(4)–O(12)	82.21(15)
O(2)–Ni(3)–N(8)	93.7(2)	O(32)–Ni(4)–N(38)	93.2(2)
O(2)–Ni(3)–O(22)	101.07(17)	O(32)–Ni(4)–O(12)	101.59(17)
N(8)–Ni(3)–O(10)	83.7(2)	N(38)–Ni(4)–O(40)	83.7(2)
O(10)–Ni(3)–O(22)	82.77(16)	O(12)–Ni(4)–O(40)	82.34(15)
Ni(1)–O(12)–Ni(2)	103.08(16)	Ni(2)–O(22)–Ni(3)	97.56(16)
Ni(1)–O(22)–Ni(2)	103.76(16)	Ni(2)–O(40)–Ni(3)	94.97(16)
Ni(1)–O(10)–Ni(3)	103.00(17)	Ni(2)–O(12)–Ni(4)	96.72(15)
Ni(1)–O(22)–Ni(3)	96.49(15)	Ni(2)–O(40)–Ni(4)	104.37(18)
Ni(1)–O(10)–Ni(4)	94.88(16)	Ni(3)–O(10)–Ni(4)	96.60(16)
Ni(1)–O(12)–Ni(4)	96.70(17)	Ni(3)–O(40)–Ni(4)	97.11(16)

Like the similarity between the geometry of Ni(1) and Ni(2), the coordination environments of Ni(3) and Ni(4) are also similar. In these cases, each metal centre is coordinated to two μ_3-alkoxido oxygen atoms [O(10) and O(40)], one μ_3-phenoxido oxygen [O(22) for Ni(3) and O(12) for Ni(4)], one monodentate phenoxido oxygen [O(2) for Ni(3) and O(32) for Ni(4)], one imine nitrogen [N(8) for Ni(3) and N(38) for Ni(4)] and one methoxy oxygen [O(21) for Ni(1) and O(11) for Ni(4)]. The coordination environment of these two metal centres is significantly distorted octahedral, in which N(8)O(10)O(22)O(2) and N(38)O(40)O(12)O(32) are the basal planes for metal centres Ni(3) and Ni(4), respectively. The average deviation of the constituent atoms and the displacement of the metal ion from the least-squares basal planes are ca. 0.14 Å and ca. 0.05 Å. In these cases also, the similar metal–ligand contacts have almost identical values. The *trans* angles [154.73(16)–174.55(18)°] and the wide ranges of the *cis* angles [73.25(15)–109.19(19)°] are indicative of significant distortion of the coordination environment of Ni(3) and Ni(4). The greater distortion for Ni(3) and Ni(4) than that of Ni(1) and Ni(2) is also evident from the above-mentioned metrical parameters.

Of the 12 edges of the Ni_4O_4 cubane, the 2 edges Ni(1)–O(22) and Ni(2)–O(12) are significantly longer [2.265(4) and 2.281(4) Å, respectively] relative to the 10 other edges, which lie in the range 2.007(6)–2.090(4) Å (Table 2). The internal angles Ni–O–Ni and O–Ni–O lie in the ranges 94.88(16)–104.37(18)° and 75.81(15)–82.89(15)°. All in all, the Ni_4O_4 core is a distorted cubane.

Inasmuch as the bridges play dominating roles in magnetic exchange interactions, it is relevant to summarize the types of bridges and bridge angles in **2**. Two metal centres are bridged in the following ways: Ni(1)···Ni(2) by two phenoxido bridges; Ni(3)···Ni(4) by two alkoxido bridges; Ni(1)···Ni(3), Ni(1)···Ni(4), Ni(2)···Ni(3) and Ni(2)···Ni(4) each by one phenoxido and one alkoxido bridge. The average bridge angles for the above pairs are 103.42, 96.85 and 98.08°, respectively.

A number of Ni_4O_4 cubane-type compounds have been reported in the literature, the majority of which are alkoxido bridged.[9–12,23] There are few examples where the bridging moieties are either of tetrakis(μ_3-phenoxido),[13,14] tetrakis(μ_3-hydroxido),[15] tetrakis(μ_3-methoxido),[16–18,23] bis(μ_3-hydroxido)bis(μ_3-alkoxido)[19,23] and bis(μ_3-phenoxido)bis(μ_3-methoxido).[20,23] There is only one example where all the bridges (hydroxido, phenoxido, alkoxido and oxido) are different.[21] To the best of our knowledge, compound **2**, in which the Ni_4O_4 cubane core is composed by two μ_3-phenoxido and two μ_3-alkoxido moieties, represents the sole example of this type.

Magnetic Properties of 1 and 2

DC magnetic susceptibility data were collected for a crushed crystalline compound of **1** at an applied magnetic field of 0.7 T in the 2 to 300 K temperature range. The data are shown in Figure 4 as a $\chi_M T$ vs. T plot. The $\chi_M T$ value at 300 K is 2.58 $cm^3 K mol^{-1}$, slightly above that expected

for two noninteracting Ni^{II} centres with $S = 1$ and $g = 2.2$. As the temperature was decreased, the $\chi_M T$ product increased until it reached a maximum value of 3.06 $cm^3 K mol^{-1}$ at 15 K. Below this temperature, the $\chi_M T$ product constantly dropped to a value of 1.77 $cm^3 K mol^{-1}$ at 2 K. The experimental data were fitted by using the MAGPACK program [25] with the exchange Hamiltonian $\hat{H} = -2J[\hat{S}_1\hat{S}_2] + \Sigma D\hat{S}_{iz}^2$. This simulation also takes into account the single-ion anisotropy of each metal centre in the cluster. The best-fitting parameters were $g = 2.24$, $J = 3.33\ cm^{-1}$ and $D(Ni1) = D(Ni2) = |6.68|\ cm^{-1}$ ($R = 0.23 \times 10^{-3}$), resulting in a spin ground state of $S_T = 2$ for dinuclear complex **1**. Intermolecular interactions through H-bonds (Figure S1, Supporting Information) with the solvated water molecules were included in the model by using mean field theory and the best fitting, which gave $z'J' = -0.29\ cm^{-1}$. The field dependence of the magnetization for **1** was also studied at 2 K and is shown in Figure 5. Saturation is not fully reached at 5 T and the curve does not conform to a Brillouin model as a result of the inherent single-ion anisotropy of Ni^{II}. The fitting parameters obtained from the susceptibility data were used to simulate the magnetization with the MAGPACK software, which gave a good agreement between the calculated and experimental data. The curve is shown in Figure 5 as a solid line. Fitting of the susceptibility data were also done without taking the single-ion anisotropies into account; however, these failed to model properly the low-temperature region of the susceptibility curve and the magnetization data.

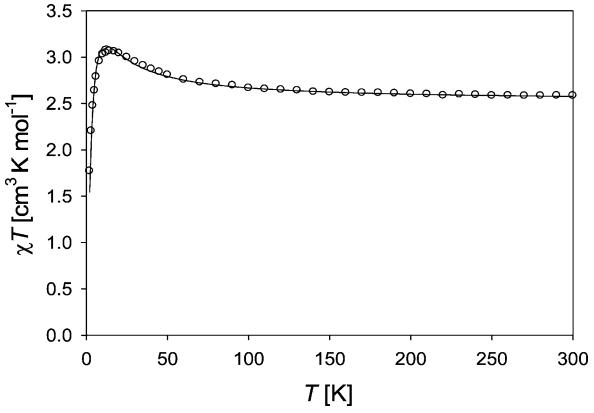

Figure 4. $\chi_M T$ (circles) vs. T plot for $[Ni^{II}_2(HL)_3(\mu\text{-}NCO)]\cdot 2H_2O$ (**1**). The solid line is the best-fit line to the experimental data, see text for fitting parameters.

We are aware of only two cases where μ-O-μ-N(isocyanate) dinickel(II) units have been reported and both of these have a μ-O(phenoxido)-$\mu_{1,1}$-N(isocyanate) bridging core.[8] One of these compound, that is, **3**, is a discrete dinuclear having bridge angles of 110.45 and 96.19° for the phenoxido and isocyanate moieties, respectively.[8a] In this case, the metal centres are ferromagnetically exchange coupled with $J = 6.2\ cm^{-1}$. The second compound is a carbonate-bridged dimer of μ-phenoxido-$\mu_{1,1}$-isocyanate dinickel(II) units and

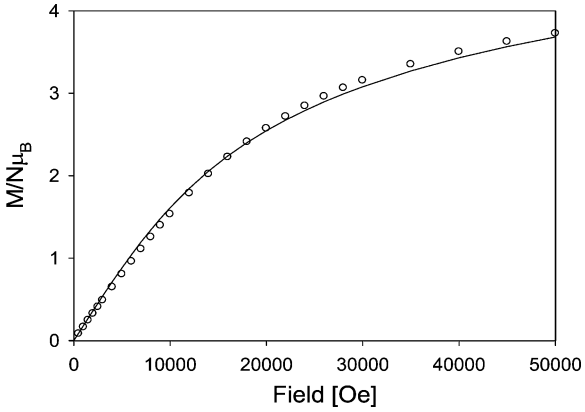

Figure 5. Magnetization (circles) vs. field plot for $[Ni^{II}_2(HL)_3(\mu\text{-}NCO)]\cdot 2H_2O$ (**1**) at 2 K. The solid lines represent the simulated curves.

the Ni–phenoxido–Ni and Ni–isocyanate–Ni angles are ca. 101 and 99.5°, respectively.[8b] Surprisingly, this compound was reported to be magnetically noninteracting.

While considering magnetic exchange interactions in heterobridged systems, the bridge angles for both the exchange pathways should be taken into consideration. It is generally held that if the Ni-phenoxido-Ni bridge angle is greater than 97°, antiferromagnetic behaviour is expected.[2b] In contrast, ferromagnetic exchange is reported in $\mu_{1,1}$-N(isocyanate) bridged compounds when the bridge angle is less than 100°.[2c,7f] In compound **1**, the phenoxido bridge angle is 106.5°, whereas the isocyanate bridge angle is 94.1°. Thus, for the two pathways J values of different signs are expected. However, it is not possible to predict a priori which particular exchange pathway will be dominating. In the other reported dinuclear Ni(μ-phenoxido)($\mu_{1,1}$-isocyanate)-Ni compound,[8a] the phenoxido bridge angle is 110.5° and the isocyanate bridge angle is 96.2°. The overall interaction in this compound is weakly ferromagnetic, as is the case with compound **1**. Again, in the reported dimer of dinuclear Ni(μ-phenoxido)($\mu_{1,1}$-isocyanate)Ni units,[8b] both the ferromagnetic (isocyanate bridge angle is 99.5°) and antiferromagnetic pathways (phenoxido bridge angle 101°) should be weaker and both are balanced to result in noninteracting metal centres.

DC magnetic susceptibility data were collected for a crushed crystalline sample of **2** at an applied magnetic field of 1 T in the 2 to 300 K temperature range. The data are shown in Figure 6 as a $\chi_M T$ vs. T plot. The $\chi_M T$ value at 300 K is 5.40 $cm^3 K mol^{-1}$, slightly above that expected for four noninteracting Ni^{II} centres with $S = 1$ and $g = 2.2$. As the temperature was decreased, the $\chi_M T$ product increased until it reached a maximum value of 7.5 $cm^3 K mol^{-1}$ at 18 K. Below this temperature, the $\chi_M T$ product constantly dropped to a value of 3.2 $cm^3 K mol^{-1}$ at 2 K. The field dependence of the magnetization for **2** at 2 K was also studied, and it is shown in Figure 7. As can be observed, the data tends to saturation at 5 T, with a $M/N\mu_B$ value of 6.2. This seems to indicate an intermediate spin value of $S_T = 3$ for tetranuclear Ni^{II} cluster **2**. AC magnetic suscep-

tibility for **2** was also studied, given the nonzero spin ground state and the known anisotropy of Ni^{II} complexes. No signals were observed in the AC magnetic susceptibility measurement as a result of the lack of a barrier for the reversal of the magnetization in **2**. This could be due to small or positive anisotropy of the Ni^{II} tetranuclear cluster.

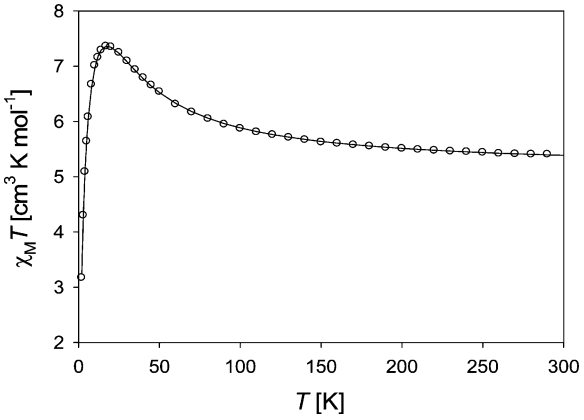

Figure 6. $\chi_M T$ (circles) vs. T plots for $[Ni^{II}_4(L)_2(HL)_2(SeCN)_2(H_2O)_2]\cdot C_3H_7NO\cdot 4H_2O$ (**2**). The solid lines represent the simulated curves.

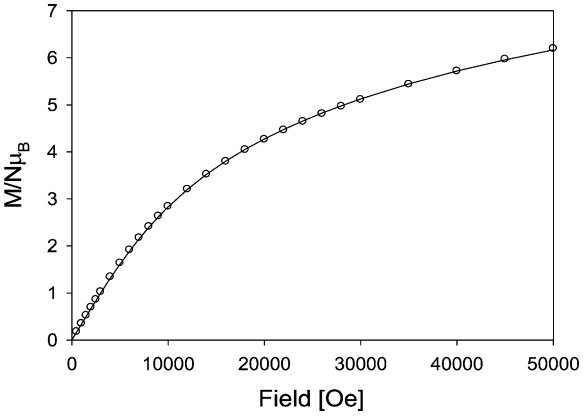

Figure 7. Magnetization (circles) vs. field plots for $[Ni^{II}_4(L)_2(HL)_2(SeCN)_2(H_2O)_2]\cdot C_3H_7NO\cdot 4H_2O$ (**2**) at 2 K. The solid line is a simulation.

As already mentioned, there are three sets of nickel(II) pairs, and therefore, the magnetic behaviour can be modelled by three different exchange integrals (Scheme 2), for which the spin Hamiltonian, taking into account the individual single-ion anisotropies, is given by:

$\hat{H} = -2J(1\text{–}2)(\hat{S}_1\hat{S}_2) - 2J(3\text{–}4)(\hat{S}_3\hat{S}_4) - 2J(\hat{S}_1\hat{S}_3 + \hat{S}_1\hat{S}_4 + \hat{S}_2\hat{S}_3 + \hat{S}_2\hat{S}_4) + \Sigma D\hat{S}_{iz}^2$

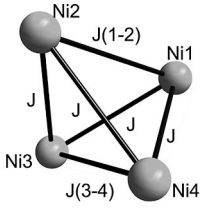

Scheme 2. Model for exchange coupling in **2**.

where $J(1\text{–}2)$ is the coupling constant between Ni(1) and Ni(2), $J(3\text{–}4)$ is the coupling constant between Ni(3) and Ni(4) and J is the coupling constant between Ni(1) and Ni(3), Ni(1) and Ni(4), Ni(2) and Ni(3) and Ni(2) and Ni(4). This Hamiltonian was used to fit the experimental data with the MAGPACK[25] software and the best-fitting parameters with a fixed g value of $g = 2.25$ were $J(1\text{–}2) = -5.14\ cm^{-1}$, $J(3\text{–}4) = 6.87\ cm^{-1}$ and $J = 4.62\ cm^{-1}$ and $D = |6.69|\ cm^{-1}$, The agreement between the experimental and calculated data is excellent ($R = 0.16 \times 10^{-1}$). With the obtained exchange parameters, the spin ground state of complex **2** is the intermediate spin $S_T = 3$. It should be noted, however, that the first excited state with $S_T = 4$ is only $2\ cm^{-1}$ above the ground state.

The exchange parameters obtained from the susceptibility data were used to simulate the magnetization at 2 K by using the MAGPACK package. These parameters provide a good simulation of the magnetization data, shown as a solid line in Figure 7. Similarly to our studies on complex **1**, the magnetic data were fitted with a two-J model and without taking into account the single-ion anisotropies. These models failed to model properly both the susceptibility and the magnetization with the same parameters and were thus discarded.

The most important parameter to govern the sign and magnitude of exchange interaction of the Ni_4O_4 cubane cores is the Ni–O–Ni angle; the interaction is ferromagnetic when this angle is close to orthogonality, whereas an antiferromagnetic interaction is observed for bridging angles larger than 99°.[9–20] Accordingly, all the interactions in some Ni_4O_4 cubanes are ferromagnetic leading to an $S_T = 4$ spin ground state,[9,16] whereas the existence of both ferro- and antiferromagnetic interactions in some systems results in either an $S_T = 4$[10,17,20] or $S_T = 0$ ground states.[13,19] In **2**, the average Ni(1)–O–Ni(2) angle is 103.42°; therefore, an antiferromagnetic interaction between Ni(1) and Ni(2) is expected. The average value of the Ni(3)–O–Ni(4) angle is 96.85°, which predicts a weak ferromagnetic interaction between Ni(3) and Ni(4). Again, as the average bridge angle between the metal ions in other pairs is 98.08°, the interaction should be weak ferromagnetic. In keeping with these expectations, the exchange coupling constants obtained in **2** are $J(1\text{–}2) = -5.14\ cm^{-1}$, $J(3\text{–}4) = 6.87\ cm^{-1}$ and $J = 4.62\ cm^{-1}$.

Conclusions

The aim of the present study was to design ferromagnetically coupled heterobridged systems through the simultaneous bridging abilities of the phenoxido and alkoxido groups in the ligand *N*-(2-hydroxyethyl)-3-methoxysalicylaldimine (H_2L) along with the bridging abilities of the cyanate and selenocyanate co-ligands. Two new heterobridged compounds $[Ni^{II}_2(HL)_3(\mu_{1,1}\text{-}NCO)]\cdot 2H_2O$ (**1**) and $[Ni^{II}_4(L)_2(HL)_2(SeCN)_2(H_2O)_2]\cdot C_3H_7NO\cdot 4H_2O$ (**2**) were isolated and structurally characterized. Whereas **1** is a heterobridged μ-phenoxido-$\mu_{1,1}$-NCO dinickel(II) compound, **2** is a hetero-

bridged bis(μ_3-phenoxido)bis(μ_3-alkoxido)tetranickel(II) system containing the $Ni^{II}_4O_4$ cubane-type core. Interestingly, the bis(μ_3-phenoxido)bis(μ_3-alkoxido) moiety in compound **2** is the sole example of this type in the $Ni^{II}_4O_4$ cubane family. It may be noted that even in Ni_4O_4 cubane-type compounds derived from Schiff base ligands similar to H_2L, the four metal ions are bridged by four alkoxido oxygen atoms.[10,11b,12] The magnetic properties of the two compounds were studied. In **1**, the exchange interactions involving the heterobridged pathways lead to overall weak ferromagnetic behaviour with an $S_T = 2$ ground state. In contrast, complex **2** has competing antiferromagnetic and ferromagnetic interactions, which result in an unusual spin ground state of $S_T = 3$. The observation of ferromagnetism in both **1** and **2** shows that the synthetic strategy and ligand design were successful in achieving ferromagnetically coupled heterobridged complexes.

Experimental Section

Materials and Physical Methods: All reagents and solvents were purchased from commercial sources and used as received. The Schiff base ligand (H_2L), which was used previously by us to derive a diuranyl(VI) compound, was synthesized following the reported procedure.[22] Elemental (C, H and N) analyses were performed with a Perkin–Elmer 2400 II analyzer. IR spectra were recorded in the region 400–4000 cm^{-1} with a Perkin–Elmer RXIFT spectrophotometer with samples as KBr disks. Variable-temperature magnetic susceptibility and magnetization measurements were carried out with a Quantum Design MPMS SQUID magnetometer. Diamagnetic corrections were estimated from the Pascal constants. *R* is the agreement factor defined as $\Sigma[(\chi_M T)_{expt.} - (\chi_M T)_{calcd.}]^2/\Sigma[(\chi_M T)_{expt.}]^2$.

$[Ni^{II}_2(HL)_3(\mu_{1,1}\text{-NCO})]\cdot 2H_2O$ (1): To a stirred *N*,*N*′-dimethylformamide (dmf) solution (5 mL) of H_2L (0.195 g, 1 mmol) was added dropwise a dmf solution (3 mL) of nickel(II) perchlorate hexahydrate (0.250 g, 0.68 mmol), and to the resulting yellowish green solution was added dropwise a dmf solution (2 mL) of triethylamine (0.202 g, 2 mmol). The colour of the solution changed to deep green. After 1 h, an aqueous solution (5 mL) of NaOCN (0.045 g, 0.68 mmol) was added dropwise to the stirred solution. After stirring for an additional 2 h, the deep-green solution was filtered to remove any suspended particles and water (10 mL) was added to it. The solution was kept at room temperature. After 2 d, a green crystalline compound containing diffractable crystals was collected by filtration and washed with water. Yield: 0.220 g (85%). $C_{31}H_{39}N_4Ni_2O_{12}$ (774.06): calcd. C 47.92, H 5.06, N 7.21; found C 47.70, H 5.12, N 7.32. FTIR (KBr): $\tilde{\nu}$ = 3396 [w, $\nu(H_2O)$], 2181 [vs, ν(OCN)], 1637 [vs, ν(C=N)] cm^{-1}.

$[Ni^{II}_4(L)_2(HL)_2(SeCN)_2(H_2O)_2]\cdot C_3H_7NO\cdot 4H_2O$ (2): A dmf solution (2 mL) of nickel(II) perchlorate hexahydrate (0.366 g, 1 mmol) was added to a stirred dmf solution (3 mL) of H_2L (0.195 g, 1 mmol). To the resulting yellowish green solution was added a dmf solution (2 mL) of triethylamine (0.202 g, 2 mmol). The colour of the solution changed to deep green. After 30 min, an aqueous solution (5 mL) of KSeCN (0.115 g, 0.8 mmol) was added dropwise to the solution with stirring. Within 15 min a green precipitate started to appear, which was dissolved by dropwise addition of a required amount of dmf. The resulting green solution was filtered to remove any suspended particles, and the filtrate was kept at room temperature. After a few days, a green crystalline compound containing diffractable single crystals was collected by filtration and washed with water. Yield: 0.280 g (80%). $C_{45}H_{65}N_7Ni_4O_{19}Se_2$ (1392.74): calcd. C 38.59, H 4.68, N 7.00; found C 39.28, H 4.75, N 7.11. FTIR (KBr): $\tilde{\nu}$ = 3334 [m, $\nu(H_2O)$], 2112 [vs, ν(SeCN)], 1630 [vs, ν(C=N)] cm^{-1}.

Crystal Structure Determination of 1 and 2: The crystallographic data of these two compounds are summarized in Table 3. Diffraction data were collected with an Enraf–Nonius CAD4 diffractometer at 293 K with data collection and reduction by using the CAD4 Express Enraf–Nonius programs package and XCAD4. All data were corrected for Lorentz polarization effects. Both structures were solved by direct methods by using SIR92[24a] and refined by least-squares methods on F^2 by using SHELXL-97.[24b] Hydrogen atoms were inserted at calculated positions with isotropic thermal parameters and refined. The hydrogen atoms of the water molecules were not located from difference Fourier map. The O(W2) and O(W3) oxygen atoms in **1** and the C(37) and C(56) carbon atoms in **2** were statically or dynamically disordered and solved. The final refinement converged to R_1 [$I > 2\sigma(I)$] values 0.0610 and 0.0538 for **1** and **2**, respectively. CCDC-715539 (for **1**) and -715540 (for **2**) contain the supplementary crystallographic data for this paper. These data can be obtained free of charge from The Cambridge Crystallographic Data Centre via www.ccdc.cam.ac.uk/data_request/cif.

Table 3. Crystallographic information for **1** and **2**.

	1	**2**
Formula	$C_{31}H_{36}N_4O_{12}Ni_2$	$C_{45}H_{57}N_7O_{19}Se_2Ni_4$
Formula weight	774.06	1392.74
Crystal system	triclinic	monoclinic
Space group	$P\bar{1}$	$P2_1/c$
a [Å]	10.135(2)	17.852(3)
b [Å]	11.521(3)	14.105(2)
c [Å]	15.239(3)	22.997(5)
α [°]	91.84(2)	90.00
β [°]	96.02(2)	95.75(2)
γ [°]	95.47(2)	90.00
V [Å^3]	1759.9(7)	5761.6(18)
Z	2	4
$D_{calcd.}$ [g cm^{-3}]	1.461	1.606
Temperature [K]	293(2)	293(2)
2θ [°]	4.06–55.00	4.04–60.24
μ [mm^{-1}]	1.135	2.625
F(000)	810	2832
Index ranges	$-13 \le h \le 13$	$-25 \le h \le 25$
	$0 \le k \le 14$	$-19 \le k \le 19$
	$-19 \le l \le 19$	$-32 \le l \le 32$
Reflections collected	8461	33787
Independent reflections	8060	16832
(R_{int})	(0.0808)	(0.3741)
R_1[a]/wR_2[b] [$I > 2\sigma(I)$]	0.0610/0.1485	0.0538/0.0964
R_1[a]/wR_2[b] (all data)	0.3099/0.2229	0.3426/0.1494

[a] $R_1 = [\Sigma||F_o| - |F_c||/\Sigma|F_o|]$. [b] $wR_2 = [\Sigma w(F_o^2 - F_c^2)^2/\Sigma wF_o^4]^{1/2}$.

Supporting Information (see footnote on the first page of this article): 2D hydrogen-bonded network and geometries of the hydrogen bonds in **1**.

Acknowledgments

Financial support from the Department of Science and Technology, Government of India (SR/S1/IC-12/2008) and Center for

Nanoscience and Nanotechnology, University of Calcutta is gratefully acknowledged. S. H. acknowledges CSIR, Government of India and R. K. acknowledges Center for Nanoscience and Nanotechnology, University of Calcutta for providing a fellowship. P. L. thanks Université Paris Descartes, Laboratoire de Cristallographie et RMN biologiques UMR 8015, Faculté de Pharmacie for single-crystal X-ray data collection. E. C. S. acknowledges the financial support of the Spanish Government (Grant CTQ2006/03949BQU and Juan de la Cierva fellowship).

[1] a) O. Kahn, *Molecular Magnetism*, VCH Publications, New York, **1993**; b) R. D. Willet, D. Gatteschi, O. Kahn (Eds.), *Magneto-Structural Correlations in Exchange Coupled Systems*, Reidel, Dordrecht, The Netherlands, **1985**; c) C. J. O'Connor (Ed.), *Research Frontiers in Magnetochemistry*, World Scientific, Singapore, **1993**; d) C. T. Chen, K. S. Suslick, *Coord. Chem. Rev.* **1993**, *128*, 293–322.

[2] a) R. Koner, H.-H. Lin, H.-H. Wei, S. Mohanta, *Inorg. Chem.* **2005**, *44*, 3524–3536; b) K. K. Nanda, L. K. Thompson, J. N. Bridson, K. Nag, *J. Chem. Soc., Chem. Commun.* **1994**, 1337–1338; c) M. I. Arriortua, R. Cortés, J. L. Mesa, L. Lezama, T. Rojo, G. Villeneuve, *Transition Met. Chem.* **1988**, *13*, 371–374.

[3] a) E. Ruiz, J. Cirera, J. Cano, S. Alvarez, C. Loose, J. Kortus, *Chem. Commun.* **2008**, 52–54; b) J. Tercero, C. Diaz, J. Ribas, J. Mahía, M. Maestro, X. Solans, *J. Chem. Soc., Dalton Trans.* **2002**, 2040–2046; c) A. Figuerola, C. Diaz, M. S. El Fallah, J. Ribas, M. Maestro, J. Mahía, *Chem. Commun.* **2001**, 1204–1205; d) A. A. Lozano, M. Sáez, J. Pérez, L. García, L. Lezama, T. Rojo, G. López, G. García, M. D. Santana, *Dalton Trans.* **2006**, 3906–3911.

[4] a) R. Winpenny (Ed.), *Single-Molecule Magnets and Related Phenomena*, Springer, Berlin, **2006**; b) J. S. Miller (Ed.), *Extended Linear Chain Compounds*, Plenum, New York, **1983**, vol. III; c) D. Gatteschi, O. Kahn, J. S. Miller, F. Palacio (Eds.), *Magnetic Molecular Materials*, Kluwer Academic Publishers, Dordrecht, **1991**; d) D. B. Amabilino, J. Veciana in *Magnetism*: *Molecules to Materials II* (Eds.: J. S. Miller, M. Drillon), Wiley-VCH, Weinheim, **2001**, pp. 1–60; e) H. Iwamura, K. Inoue in *Magnetism*: *Molecules to Materials II* (Eds.: J. S. Miller, M. Drillon), Wiley-VCH, Weinheim, **2001**, pp. 61–108.

[5] a) J. Ribas, A. Escuer, M. Monfort, R. Vicente, R. Cortés, L. Lezama, T. Rojo, *Coord. Chem. Rev.* **1999**, *193–195*, 1027–1068; b) M. Verdaguer, A. Bleuzen, V. Marvaud, J. Vaissermann, M. Seuleiman, C. Desplanches, A. Scuiller, C. Train, R. Garde, G. Galley, C. Lomenech, I. Rosenman, P. Veillet, C. Cartier, F. Villain, *Coord. Chem. Rev.* **1999**, *190–192*, 1023–1047; c) G. Rajaraman, M. Murugesu, E. C. Saudo, M. Soler, W. Wernsdorfer, M. Helliwell, C. Muryn, J. Raftery, S. J. Teat, G. Christou, E. K. Brechin, *J. Am. Chem. Soc.* **2004**, *126*, 15445–15457; d) D. Venegas-Yazigi, E. Ruiz, J. Cano, S. Alvarez, *Dalton Trans.* **2006**, 2643–2646; e) T. C. Stamatatos, V. Nastopoulos, A. J. Tasiopoulos, E. E. Moushi, W. Wernsdorfer, G. Christou, S. P. Perlepes, *Inorg. Chem.* **2008**, *47*, 10081–10089; f) T. C. Stamatatos, D. Foguet-Albiol, S.-C. Lee, C. C. Stoumpos, C. P. Raptopoulou, A. Terzis, W. Wernsdorfer, S. O. Hill, S. P. Perlepes, G. Christou, *J. Am. Chem. Soc.* **2007**, *129*, 9484–9496.

[6] a) Y.-C. Chou, S.-F. Huang, R. Koner, G.-H. Lee, Y. Wang, S. Mohanta, H.-H. Wei, *Inorg. Chem.* **2004**, *43*, 2759–2761; b) V. McKee, J. V. Dagdigian, R. Bau, C. A. Reed, *J. Am. Chem. Soc.* **1981**, *103*, 7000–7001; c) W. Mazurek, B. J. Kennedy, K. S. Murray, M. J. O'Connor, J. R. Rodgers, M. R. Snow, A. G. Wedd, P. R. Zwack, *Inorg. Chem.* **1985**, *24*, 3258–3264; d) Y. Nishida, S. Kida, *J. Chem. Soc., Dalton Trans.* **1986**, 2633–2640; e) T. N. Doman, D. E. Williams, J. F. Banks, R. M. Buchanan, H.-R. Chang, R. J. Webb, D. N. Hendrickson, *Inorg. Chem.* **1990**, *29*, 1058–1062.

[7] a) T. Sato, W. Mori, Y. Xie, N. Kanehisa, Y. Kai, M. Fuji, S. Goto, E. Nagai, Y. Nakao, *Inorg. Chim. Acta* **2006**, *359*, 2271–2274; b) G. Ambrosi, P. Dapporto, M. Formica, V. Fusi, L. Giorgi, A. Guerri, M. Micheloni, P. Paoli, R. Pontellini, P. Rossi, *Dalton Trans.* **2004**, 3468–3474; c) A. K. Boudalis, J.-M. Clemente-Juan, F. Dahan, J.-P. Tuchagues, *Inorg. Chem.* **2004**, *43*, 1574–1586; d) R. Bouwman, P. Evans, R. A. G. de Graaf, H. Kooijman, R. Poinsot, P. Rabu, J. Reedijk, A. L. Spek, *Inorg. Chem.* **1995**, *34*, 6302–6311; e) J. M. Clemente-Juan, C. Mackiewicz, M. Verelst, F. Dahan, A. Bousseksou, Y. Sanakis, J.-P. Tuchagues, *Inorg. Chem.* **2002**, *41*, 1478–1491; f) M. G. Barandika, Z. Serna, R. Cortés, L. Lezama, T. Rojo, M. K. Urtiaga, M. I. Arriortua, *Chem. Commun.* **2001**, 45–46.

[8] a) S. K. Dey, N. Mondal, M. S. E. Fallah, R. Vicente, A. Escuer, X. Solans, M. Font-Barda, T. Matsushita, V. Gramlich, S. Mitra, *Inorg. Chem.* **2004**, *43*, 2427–2434; b) S. Uozumi, H. Furutachi, M. Ohba, H. Ōkawa, D. E. Fenton, K. Shindo, S. Murata, D. J. Kitko, *Inorg. Chem.* **1998**, *37*, 6281–6287.

[9] a) F. Paap, E. Bouwman, W. L. Driessen, R. A. G. de Graaff, J. Reedijk, *J. Chem. Soc., Dalton Trans.* **1985**, 737–741; b) M. Moragues-Cánovas, M. Helliwell, L. Ricard, É. Rivière, W. Wernsdorfer, E. Brechin, T. Mallah, *Eur. J. Inorg. Chem.* **2004**, 2219–2222; c) E.-C. Yang, W. Wernsdorfer, L. N. Zakharov, Y. Karaki, A. Yamaguchi, R. M. Isidro, G.-D. Lu, S. A. Wilson, A. L. Rheingold, H. Ishimoto, D. N. Hendrickson, *Inorg. Chem.* **2006**, *45*, 529–546; d) E.-C. Yang, W. Wernsdorfer, S. Hill, R. S. Edwards, M. Nakano, S. Maccagnano, L. N. Zakharov, A. L. Rheingold, G. Christou, D. N. Hendrickson, *Polyhedron* **2003**, *22*, 1727–1734; e) J. Lawrence, E.-C. Yang, R. Edwards, M. M. Olmstead, C. Ramsey, N. S. Dalal, P. K. Gantzel, S. Hill, D. N. Hendrickson, *Inorg. Chem.* **2008**, *47*, 1965–1974; f) J.-W. Ran, S.-Y. Zhang, B. Xu, Y. Xia, D. Guo, J.-Y. Zhang, Y. Li, *Inorg. Chem. Commun.* **2008**, *11*, 73–76; g) A. Escuer, M. Font-Bardía, S. B. Kumar, X. Solans, R. Vicente, *Polyhedron* **1999**, *18*, 909–914.

[10] C. Boskovic, E. Rusanov, H. Stoeckli-Evans, H. U. Güdel, *Inorg. Chem. Commun.* **2002**, *5*, 881–886.

[11] a) G. S. Papaefstathiou, A. Escuer, F. A. Mautner, C. Raptopoulou, A. Terzis, S. P. Perlepes, R. Vicente, *Eur. J. Inorg. Chem.* **2005**, 879–893; b) S. Akine, A. Akimoto, T. Shiga, H. Oshio, T. Nabeshima, *Inorg. Chem.* **2008**, *47*, 875–885.

[12] B. F. Abrahams, T. A. Hudson, R. Robson, *Chem. Eur. J.* **2006**, *12*, 7095–7102.

[13] G. Aromí, A. S. Batsanov, P. Christian, M. Helliwell, O. Roubeau, G. A. Timco, R. E. P. Winpenny, *Dalton Trans.* **2003**, 4466–4471.

[14] A. J. Atkins, A. J. Blake, M. Schroder, *J. Chem. Soc., Chem. Commun.* **1993**, 1662–1665.

[15] a) L. Ballester, E. Coronado, A. Gutiérrez, A. Mange, M. F. Perpiñán, E. Pinilla, T. Rico, *Inorg. Chem.* **1992**, *31*, 2053–2056; b) J. P. Wikstrom, A. Y. Nazarenko, W. M. Reiff, E. V. Rybak-Akimova, *Inorg. Chim. Acta* **2007**, *360*, 3733–3740.

[16] a) M. S. E. Fallah, E. Rentschler, A. Caneschi, D. Gatteschi, *Inorg. Chim. Acta* **1996**, *247*, 231–235; b) G. Chaboussant, R. Basler, H.-U. Güdel, S. Ochsenbein, A. Parkin, S. Parsons, G. Rajaraman, A. Sieber, A. A. Smith, G. A. Timco, R. E. P. Winpenny, *Dalton Trans.* **2004**, 2758–2766.

[17] T. K. Paine, E. Rentschler, T. Weyhermüller, P. Chaudhuri, *Eur. J. Inorg. Chem.* **2003**, 3167–3178.

[18] a) Z. Lin, Z. Li, H. Zhang, *Cryst. Growth Des.* **2007**, *7*, 589–591; b) W. L. Gladfelter, M. W. Lynch, W. P. Schaefer, D. N. Hendrickson, H. B. Gray, *Inorg. Chem.* **1981**, *20*, 2390–2397.

[19] J. M. Clemente-Juan, B. Chansou, B. Donnadieu, J.-P. Tuchagues, *Inorg. Chem.* **2000**, *39*, 5515–5519.

[20] S. Mukherjee, T. Weyhermüller, E. Bothe, K. Wieghardt, P. Chaudhuri, *Eur. J. Inorg. Chem.* **2003**, 863–875.

[21] S. Cromie, F. Launay, V. McKee, *Chem. Commun.* **2001**, 1918–1919.

[22] S. Hazra, S. Majumder, M. Fleck, S. Mohanta, *Polyhedron* **2008**, *27*, 1408–1414.

[23] Those systems are considered here as alkoxido-bridged, where the alkoxido moiety comes from the chelating ligand, whereas

compounds in which the metal centres are bridged by deprotonated methanol are classified here as methoxido-bridged.

[24] a) A. Altomare, G. Cascarano, C. Giacovazzo, A. Guagliardi, M. C. Burla, G. Polidori, M. Camalli, *J. Appl. Crystallogr.* **1994**, *27*, 435–436; b) G. M. Sheldrick, *SHELXL-97*: *A Program for Crystal Structure Refinement*, University of Göttingen, Göttingen, Germany, **1997**.

[25] J. J. Borrás-Almenar, J. M. Clemente-Juan, E. Coronado, B. S. Tsukerblat, *Inorg. Chem.* **1999**, *38*, 6081–6088.

Received: April 18, 2009
Published Online: July 7, 2009

